

RSC Advances



This is an *Accepted Manuscript*, which has been through the Royal Society of Chemistry peer review process and has been accepted for publication.

Accepted Manuscripts are published online shortly after acceptance, before technical editing, formatting and proof reading. Using this free service, authors can make their results available to the community, in citable form, before we publish the edited article. This *Accepted Manuscript* will be replaced by the edited, formatted and paginated article as soon as this is available.

You can find more information about *Accepted Manuscripts* in the [Information for Authors](#).

Please note that technical editing may introduce minor changes to the text and/or graphics, which may alter content. The journal's standard [Terms & Conditions](#) and the [Ethical guidelines](#) still apply. In no event shall the Royal Society of Chemistry be held responsible for any errors or omissions in this *Accepted Manuscript* or any consequences arising from the use of any information it contains.

Potential-gated molecularly imprinted smart electrode for nicotinamide analysis

Najmeh Karimian^{a,b}, Mohammad Hossein Arbab Zavar^b, Mahmoud Chamsaz^b, Narges Ashraf^b, Anthony P.F. Turner^a and Ashutosh Tiwari^{a,c*}

^a*Biosensors and Bioelectronics Centre, Department of Physics, Chemistry and Biology (IFM), Linköping University, S-58183 Linköping, Sweden*

^b*Department of Chemistry, Faculty of Sciences, Ferdowsi University of Mashhad, Mashhad, Iran*

^c*Tekidag AB, Mjärdevi Science Park, Teknikringen 4A, SE 583 30 Linköping, Sweden*

*Corresponding author.

Tel: (+46) 1328 2395; Fax: (+46) 1313 7568; E-mail: ashutosh.tiwari@liu.se

Abstract

Triggered surface responsiveness paves the way for smart sensor technologies that not only have tunable retention, but also provide sensing through a ‘built-in’ programming of electrode material. In this study, we report a potential-gated electrochemical sensor for determination of nicotinamide (NAM) based on a molecularly imprinted overoxidised polypyrrole electrode. The sensitive layer was prepared by electropolymerisation of pyrrole on a glassy carbon electrode in the presence of NAM as a template molecule, followed by alkali extraction. Electrochemical methods were used to monitor the processes of electropolymerisation, template removal and binding in the presence of a $[\text{Fe}(\text{CN})_6]^{3-}/[\text{Fe}(\text{CN})_6]^{4-}$ redox couple as an electrochemical probe. Several factors affecting the performance of the MIP-modified electrode were investigated and optimized. The peak current of ferro/ferricyanide couple decreased linearly with successive addition of NAM in the concentration ranging from 0.9×10^{-6} to 9.9×10^{-3} M with a detection limit of 1.7×10^{-7} M (S/N = 3). The molecularly-imprinted polymer (MIP) electrode had excellent recognition capability for NAM compared to structurally related molecules. Moreover, the reproducibility and repeatability of the NAM-imprinted electrode were all found to be satisfactory. The results from sample analysis confirmed the applicability of the NAM-imprinted electrode to reusable quantitative analysis in commercial pharmaceutical samples.

Keywords: Smart molecularly imprinting, triggered surfaces, potential-gated molecularly-imprinted polymer electrode, nicotinamide sensor.

1. Introduction

Development of advanced electrode materials with smart properties is a key component for the future of electroanalysis.¹ A wide variety of permutations of functional properties have been directed towards progressing cutting-edge mimetic materials, thus producing a plethora of high-performance sensors, smart surfaces and probes. Responsive materials have commanded significant attention in recent years due to their unique tunable affinity and adjustable binding properties upon receiving stimuli.^{2,3} Novel approaches include on/off-switchable or tunable surfaces triggered by changes in temperature, pH, light intensity, magnetic field and potential for analytics. However, most of the stimuli have been restricted to light, magnetic field and pH.^{4,5} Despite the successes of smart systems, however, there is a steadily growing interest in smart recognition systems using synthetic analogs, which offer improved stability, cost-effectiveness and means of rapid fabrication. Potential-controlled molecularly imprinted electrodes could provide a promising alternative and direct approach to determine a template using tunable imprinted electrodes.

Electroactive polymers have attracted wide spread attention in the design of sensors.⁶ The most important aspect of a conjugated polymers from an electrochemical point of view, is their ability to act as an electronic conductor. This property is further enhanced by redox switching at specific potentials accompanied by the movement of dopant ions into or out of the material depending on net polymer charge.⁷ The biocompatibility, electrochemical redox activity even in neutral pH solution⁸, improved mechanical properties (e.g., polypyrrole films, PPy) and the interfacial control of their properties by the application of potential-triggers, makes them interesting candidates for design and synthesis of a new, smarter molecularly-imprinted polymer. Overoxidation of conducting polymers, notably PPy, where the polymer is held above the

standard oxidative potential, leads to loss of conductivity and de-doping.⁷ Overoxidised polypyrrole has already been used in a number of electroanalytical applications; the overoxidised film works as a porous electrode coating, which has cation-exchange and molecular sieve properties.⁹

Molecularly imprinted polymers (MIPs) are promising materials currently being explored extensively as recognition elements or modifying agents for sensors.¹⁰⁻¹⁴ Among different methods for synthesis of MIPs, electrochemical synthesis is preferred for research purposes due to the simplicity of the technique, control over material thickness, geometry, precise location, the facility to trap target in the structure during synthesis and the generation of good quality films.⁷ The specific combination of molecular imprinting with a potential-gated molecularly-imprinted polymer electrode is of considerable interest due to its potential to generate sensors with high stability and selectivity, simple operation, low cost and high binding affinity comparable to a biological receptor.¹⁰⁻¹⁴ This new generation of smart materials may also find application in other niche areas such as biosensors and drug delivery.

Nicotinamide (3-pyridine carboxylic acid amide, NAM), a water-soluble amide form vitamin B₃, is both a food nutrient and a drug that has an important role during cellular energy management and metabolic disorders such as *Diabetes Mellitus*.¹⁵ It also aids proper circulation and healthy skin, functioning of the nervous system and normal secretion of bile and stomach fluid. Hence, it is a pharmacologically important compound.¹⁶ It functions as the precursor for the coenzymes nicotinamide adenine dinucleotide (NAD) and nicotinamide adenine dinucleotide phosphate (NADP) coenzymes. Consequently, it is involved in more than 200 redox enzyme reactions in the human body.¹⁷ Furthermore, in deficiency states, lack of NAM can lead to fatigue, loss of appetite, pigmented rashes of the skin and oral ulcerations. More severe states of

deficiency lead to *Pellagra*.¹⁵ While excessive NAM may also be detrimental.¹⁶ NAM is found naturally in sources such as animal products, legumes and cereals composed of whole grains. Hence, the estimation of NAM is of great importance. Nicotinamide reduces at a potential in aqueous media very near to that of background discharge reaction on solid electrodes,^{16, 18} which makes it difficult to study on solid electrodes. So, electrode modification has a great importance in electrochemistry as it enhances the sensitivity and specificity of analyte determination.

To the best of our knowledge, there is no previous report on potential-gated molecularly-imprinted smart electrodes for the selective determination of nicotinamide. Thus, we propose that a viable route to achieve the necessary enhanced performance is by using a “smart” mimetic electrode for both fundamental and applied studies of high-performance analytical devices. Therefore, we report herein, the fabrication of an electrochemical nicotinamide (NAM) sensor based on electropolymerised molecularly-imprinted overoxidised polypyrrole (OPPy), exploiting electrochemical polymerisation of pyrrole monomer together with target NAM molecules on a glassy carbon electrode. The analytical performance of the sensor was evaluated by electrochemical methods. Under optimised conditions, the experimental results showed that the smart MIP electrode possessed fast rebinding dynamics and an excellent recognition capacity for NAM.

2. Experimental section

2.1. Materials

Pyrrole (Py, $\geq 95\%$) and 4-amino-benzoic acid, thiamine hydrochloride (vitamin B₁), riboflavin (vitamin B₂), pyridoxal (vitamin B₆), ascorbic acid (vitamin C), sodium perchlorate (NaClO₄); were obtained from E. Merck, Germany. Pyrrole was distilled repeatedly under vacuum until a

colorless liquid was obtained and kept in darkness at 4 °C. Nicotinamide (99.82%, Aarti Drugs Limited, Maharashtra, India), potassium ferricyanide ($K_3[Fe(CN)_6]$, BDH), potassium ferrocyanide ($K_4[Fe(CN)_6]$, Riedel, Germany) were used as received. Multivitamin tablet (B-complex) included: Nicotinamide (B3) = 20 mg, B6 = 2 mg, B2 = 2 mg, B1 = 5 mg was purchased from Health Store. $K_3[Fe(CN)_6]/K_4[Fe(CN)_6]$ (1:1, 0.5 mM) were prepared in 0.1 M KCl. All other reagents were of analytical grade and solutions were prepared using double distilled deionised water.

2.2. Instrumentation

Electrochemical measurements were performed using a SAMA electrochemical analyser (SAMA 500, Iran) controlled by software supplied by the manufacturer. A standard three-electrode configuration was used. A glassy carbon electrode (GCE, 2.0 mm diameter), a platinum wire and an Ag|AgCl|KCl (saturated) electrode were used as working electrode, counter and reference electrodes, respectively. A Metrohm 632 pH-meter (Metrohm, Switzerland) was employed for pH measurements. Scanning electron microscopy (SEM) was performed using a Leo 1450VP SEM (Germany) at 20 kV. All measurements were carried out at room temperature.

2.3. Preparation of MIP and NIP electrodes

Molecularly imprinted polymer (MIP) and non-molecularly imprinted polymer (NIP) were constructed via the electropolymerisation of pyrrole monomer. Prior to the electropolymerisation, the glassy carbon electrode was polished carefully to a mirror-like surface with 0.3~0.05 μm alumina aqueous slurry and was then alternately washed in an ultrasonic cleaner with doubly distilled water for 2 min. The electrosynthesis of imprinted OPPy film was

performed by cyclic voltammetry (16 scans, $100 \text{ mV}\cdot\text{s}^{-1}$) in the range of -0.2 to 1.7 V vs. Ag|AgCl in an aqueous solution containing 7.0 mM = NAM, 50.0 mM = pyrrole and 100.0 mM = NaClO_4 at 25°C . Before polymerisation, the solution was deoxygenated by bubbling argon gas through it for about 15 min. After the electropolymerisation, the polypyrrole modified electrodes were washed in ethanol-water (2:1, v/v) solution containing 0.1 M NaOH for 20 min under mild stirring, followed by subsequent washing with water to partially remove the template molecule entrapped in the film. For comparison of binding ability and specificity, a non-molecularly imprinted polymer modified glassy carbon electrode (NIP-GCE) was also synthesised under the same conditions in the absence of NAM. A schematic diagram of E/V triggered NAM recognition is shown in Scheme 1.

Scheme 1. Schematic representation of smart MIP surface via potentially tuned formation of the recognition site around template, NAM and specific NAM binding sites on the electrode.

2.4. Electrochemical measurements

The interaction between NAM and the smart MIP electrode was evaluated by incubating the electrode in a solution containing appropriate concentrations of NAM for 10 min with stirring. Electrochemical measurements to characterise the MIP electrode were carried out in the presence of 0.5 mM $[\text{Fe}(\text{CN})_6]^{3-}/[\text{Fe}(\text{CN})_6]^{4-}$ (1:1) solution containing 0.1 M KCl. Cyclic voltammograms (CVs) of the imprinted membranes were recorded in the potential range 0.0 to 0.6 V vs. Ag/AgCl, with a scan rate of 50 mV s^{-1} . Differential pulse voltammetry (DPV) runs for each concentration of test analyte were quantified over a potential range of 0.0 to 0.4 V at a scan rate of 50 mV s^{-1} and pulse amplitude of 25 mV. 4-Amino-benzoic acid, vitamin C together with

B-complex vitamins was selected as competitor compounds in order to evaluate the recognition specificity of the prepared smart MIP electrode. The chemical structure of NAM and a like compounds are provided in Fig. S1.

2.5. Sample preparation

A multivitamin tablet containing NAM was used to test the electrode's ability to estimate NAM. The tablet was finely powdered and then dissolved in water. The solution was sonicated for 10 min and filtered. An aliquot of appropriate volume of stock solution was transferred into 50 mL volumetric flask. In order that the concentration of NAM was in the working range the samples were further diluted. A standard addition method was used for quantitative determination of NAM by successive additions of standard NAM solution.

3. Results and discussion

Electrochemical polymerisation of pyrrole was carried out in the presence of NAM as a target and optimum conditions for preparation of electrosynthesised film were established. The binding of the target was measured electrochemically via suppression of the redox behaviour of a probe reaction at the modified electrode via potential gating. The analytical performance of the sensor was elaborated and NAM was measured in the commercial pharmaceutical tablet.

3.1. Preparation of MIP electrode

The electrochemical properties of PPy strongly depend on the redox state of this polymer.¹⁹ Overoxidation of PPy appears at more positive potentials in water and/or an oxygen-containing environment. During this process, PPy loses its electroactivity in parallel with the ejection of the

dopants and generation of oxygen-containing groups such as carbonyl and carboxyl on the polypyrrole backbone.²⁰ The electrochemical behavior of pyrrole was investigated in freshly aqueous prepared and degassed solution of 50.0 mM pyrrole, 100.0 mM NaClO₄ and 7.0 mM NAM as template, using potential cycling between -0.2 and +1.7 V vs. Ag/AgCl for 16 consecutive scans, at scan rate of potential 100 mV s⁻¹ onto a cleaned GC electrode surface. The cyclic voltammograms recorded during electrosynthesis of OPPy film are shown in Fig.1a. On the first cycle, an irreversible anodic peak was observed at ~1.1 V assigned to the oxidation of pyrrole to its radical cation, followed by the coupling of radicals and formation of polymeric film at the glassy carbon electrode surface. During continuous cycling, a decrease in conductivity at high current densities (high anodic potential) can also be caused by attack of nucleophiles, like H₂O and/or OH⁻ on the polymer backbone and consequently the appearance of carbonyl, carboxyl and hydroxyl groups that interrupt the conjugated structure and lower the intrinsic conductivity of the polymer.²⁰ The coverage of surface GCE by insulate film of OPPy is confirmed by the disappearance of the redox peaks of ferro/ferricyanide probe (inset of Fig. 1a). The same oxidation peak was observed with the electropolymerisation of the monomer alone (NIP), which means that the template was electrochemically stable over the scanned potential window and only the monomer underwent electropolymerisation (Fig. S2).

The thickness of the polymer film can be estimated from anodic oxidation peak integration by Faraday's law ($d = mQ/FA\rho$ where, d - thickness of the polymer layer, m - the molecular weight of the monomer, Q - the total charge passed during the electropolymerisation obtained by integration of the voltammogram, F - Faraday constant (96485 C mol⁻¹), A - the area of electrode surface (0.0314 cm²) and ρ - the density of PPy) revealed a growth of the polymer

layer during first eight cycles up to 88 nmol cm^{-2} , followed by a less than 1% increase during the rest of the voltammetry cycles. The thickness of the polymer film was assessed as 19.5 nm.

During the electrodeposition of pyrrole, NAM template molecules are trapped in to the polymer matrix as a result of the ability of these molecules to interact with the pyrrole units. The oxygen atom in the C=O group of the NAM molecule forms a hydrogen bond with the hydrogen atom in the N-H group of the pyrrole units. Hydrogen bonding could occur between the hydrogen in the amide group of NAM and the nitrogen atom of the pyrrole N-H groups. One of the most important elements in the fabrication of an efficient MIP-electrode is template removal. An optimal extractive solvent should strongly interact with polymer causing the swelling of the coating necessary for the template release without serious damage to the backbone of polymer.²¹ For characterisation of the polymerised films before and after template removal, a specific potential window (i.e., applied a potential gate of 0-0.4 V) was chosen. Since, NAM undergoes reduction at more negative^{16, 18} contemporarily, in the applied potential gate, PPy and NAM, both are electro-inactive in aqueous media those do not compromise the activity of ferro/ferricyanide redox probe during analysis. As an increase in permeability enable ferrocyanide to diffuse through polymer towards MIP electrode surface. This phenomenon provided an analytical signal in specified potential gate. Differential pulse voltammetry was employed to monitor the probe redox signal (Fig. 1b). After examination of various strategies and solvents, the highest difference in voltammetric signal between imprinted and non-imprinted polymers was observed after treatment in 0.1 M NaOH solution in ethanol-water (2:1 v/v) for 20 min under mild stirring, followed by subsequent washing with water to partially remove the template molecule entrapped in the film. An alkaline medium was chosen to avoid degradation of polymerised PPy films.²² The morphologies of MIP-GCE and NIP-GCE were examined using SEM, and are shown in

Figs. 1c and d. It is believed that the porosity and grain size of the electropolymerised polypyrrole are dependent on the supporting electrolyte and other experimental conditions used in the method.²³ It could be seen from the SEM images that there was difference in the morphologies between MIPs-GCE and NIPs-GCE. MIPs film formed on GCE surface was rough, but NIPs film was smooth and no cracks could be observed. In other words, NIP-GCE surface is rather compact as compared to MIP-GCE surface. The roughness of MIPs film could be attributed to the electropolymerisation of polymer film in the presence of NAM.

Figure 1. Preparation of smart MIP electrode via electropolymerisation of pyrrole and template removal; (a) cyclic voltammogram for pyrrole electropolymerisation at a glassy carbon electrode (Py: 50.0 mM, NAM: 7.0 mM, sodium perchlorate: 100.0 mM in aqueous solution, number of cycles = 16, potential range -0.2 to +1.7 V and scan rate 100 mV s⁻¹). Inset: cyclic voltammograms recorded with bare GC electrode (black solid line, -I-) and MIP-modified (red dashed line, -II-) and NIP-modified (blue pointed line, -III-) electrodes in 0.5 mM K₃Fe(CN)₆, 0.5 mM K₄Fe(CN)₆, 0.1 M KCl; and (b) differential pulse voltammograms obtained with MIP (red solid line, -I-) and NIP-modified (blue dashed line, -II-) electrodes after template removing (cf., conditions are the same as inset of Fig. 1a). SEM images of c) MIP with insets of high resolution and d) NIP electrodes.

3.2. Optimisation conditions of the MIP

In order to construct an efficient MIP sensor, different influencing factors including concentration of monomer (pyrrole), scan cycles of electropolymerisation process, concentration of template molecule (NAM), time and pH of rebinding were investigated. The change of current response of [Fe(CN)₆]³⁻/[Fe(CN)₆]⁴⁻ on each electrode was calculated by subtracting current

caused in the presence of NAM solution (15.0 μM) from the current recorded in the absence of NAM (δi_p).

The monomer concentration in the polymerisation process affects the thickness of the deposit and the amount of imprinted molecule in the polymer matrix, which in turn further affects the electrochemical behavior of the sensor.²⁴ To evaluate the effect of the pyrrole concentration on the response of MIP to NAM, the MIPs were electropolymerised in solutions of a constant NAM concentration (7.0 mM) and of varying pyrrole concentrations in the range of 25.0 to 200.0 mM. As shown in Fig. 2a, there was a decrease in the current response below 50.0 mM of pyrrole concentration, which was probably because NAM could not be captured during the electropolymerisation process. On the other hand, if the imprinted polymer membranes are too thick due to high concentration of pyrrole (above 50.0 mM) template molecules situated at the central area of the polymer membranes cannot be completely removed from polymer matrix.²⁵ Thus, it could be concluded that the optimum monomer concentration was estimated approximately 50.0 mM.

The number of cycles applied to the preparation of MIP-GCE during the electropolymerisation influences the thickness of the polymeric film.²⁵ This increase in thickness with increase in scan cycles of electropolymerisation also affects the sensitivity and linearity of the sensor. In this research, the number of scan cycles was varied from 6 to 21 to determine the optimal film thickness (Fig. 2b). Polymer films that were formed less than 16 scan cycles were found to be unstable. Higher numbers of cycles led to the formation of thicker sensing film with less accessible imprinted sites. The current response changes of $[\text{Fe}(\text{CN})_6]^{3-}/[\text{Fe}(\text{CN})_6]^{4-}$ on MIP-GCE indicated that the optimum number of polymerisation cycles was to be 16.

The quantity and quality of the molecularly imprinted polymer recognition sites is a direct function of amount of template.²³ So the concentration of template in the process of electropolymerisation was studied and the corresponding results are shown in Fig. 2c. It was observed that the largest current response changes were obtained when the concentration of NAM was 7.0 mM. With lesser amounts, because of decreasing of imprinted sites or binding cavities in the MIPs film, the current response changes decreased. However, an excessive amount of the template molecules can lead to failure in the formation of the MIP film. Therefore, based on the results, the optimum template concentration was chosen as 7.0 mM.

The incubation step is usually a simple and effective way to enhance the sensitivity of the imprinted sensor.²⁶ The time of accumulation in NAM solution using both MIP- and NIP-modified electrodes was optimised. After an elution step using extractive solvent, the imprinted PPy-GC electrode was incubated in a stirred solution containing 15.0 μ M NAM for various incubation times. The relationship between the current response changes and the rebinding time was studied over the range 2 to 30 min. As shown in Fig. 2d, increase in the incubation time resulted in the current response increasing sharply for the first 10 minutes of incubation and after that these changes were not so sizeable. The optimal incubation time for non-imprinted electrode was also studied under the same conditions. According to the results, a high current difference between the MIP and NIP electrodes was obtained after 10 minute, which could be attributed to the better site accessibility and lower mass-transfer resistance of thin MIPs film on GCE surface. Electrostatic interactions also play an important role in the recognition of the imprinting molecule.²⁴ Therefore, the pH effect of rebinding solution was investigated. For this purpose, NAM rebinding by MIP-modified electrode was investigated in solution including a constant concentration of NAM (15.0 μ M) in PBS, with the pH value ranging from 4.0 to 8.5, containing

0.5 mM $[\text{Fe}(\text{CN})_6]^{3-}/[\text{Fe}(\text{CN})_6]^{4-}$. The pH value changes of the solution had no significant effect on the rebinding of the NAM to the imprinted sites. Hence, pH 6.0 was chosen as the optimum for the rebinding of target molecules at the MIP-GCE (Fig. S3).

Figure 2. Optimization of factors affecting the performance of the smart MIP electrode; (a) effect of the pyrrole concentration on δi_p at the NAM/MIP-GCE; (b) effect of the cycles on δi_p at the NAM/MIP-GCE; (c) effect of the nicotinamide concentration on δi_p at the NAM/MIP-GCE; in the solutions containing 0.5 mM $\text{K}_3\text{Fe}(\text{CN})_6$, 0.5 mM $\text{K}_4\text{Fe}(\text{CN})_6$, 0.1 M KCl in the presence of 15.0 μM nicotinamide after 10 min incubation time. (d) effect of the time of rebinding on δi_p at the NAM/MIP-GCE and NIP-GCE (cf., conditions are the same as Fig. 2 (a-c) just after different incubation times).

3.3. Analytical performance of MIP electrode

To investigate the practicality of the MIP-GCE for the determination of NAM, the linear range and the detection limit were obtained from calibration curves. Under the optimum conditions, differential pulse voltammetry was used to monitor the ferro/ferricyanide probe response as affected by NAM binding on the MIP-modified electrode. After template removal and background response measurements, MIP-modified electrodes were dipped into solution containing of NAM in different concentrations for 10 minutes with stirring. Fig. 3a shows the decrease of redox peak currents of the ferro/ferricyanide couple for an increase of NAM concentration in binding solution. With increasing concentration, more imprinted sites were rebound with NAM. So, the electrode reaction of the ferro/ferricyanide probe was impeded by the binding of NAM with MIP. The results showed that the decrease of peak current due to $[\text{Fe}(\text{CN})_6]^{3-}/[\text{Fe}(\text{CN})_6]^{4-}$ was proportional to the logarithm of the concentration of NAM in the

range from 0.9×10^{-6} to 9.9×10^{-3} M, with a correlation coefficient of 0.999, as shown in Fig. 3b. The detection limit was determined to be 1.7×10^{-7} M (as three times the standard deviation of the blank signal). On the contrary, the decrease of peak current of $[\text{Fe}(\text{CN})_6]^{3-}/[\text{Fe}(\text{CN})_6]^{4-}$ was much lower and independent of NAM concentration when the NIP-modified electrode was used as the working electrode, owing to the lack of imprinted cavities in the polymer film (Fig. S4). The results of different methods and some other reported detection techniques for NAM determination were summarised in Table 1. In comparison with chromatographic, spectrophotometry and other electrochemical techniques and sensors, our sensor had a wider linear range or lower detection limit, indicating that the sensitivity of sensors could be improved by the MIP- modification.

The binding isotherm of the MIP-modified electrode was fitted using a model for two types of simultaneous binding (Fig. 3c): on the sites of specific recognition inside polymer film and on the surface of electrode due to non-specific adsorption:

$$i_0 - i = \frac{B_{MAX}c}{K_D + c} + N_S c$$

where c is bulk concentration of the target, B_{MAX} - maximum number of binding sites in the MIP, K_D - equilibrium dissociation constant and N_S -binding constant for nonspecific adsorption. The value K_D obtained with fitting is 7.1×10^{-7} M (R^2 0.984).

Figure 3. NAM binding with modified electrode. (a) Differential pulse voltammograms of MIP-modified electrode after 10 min of incubation in different NAM concentrations ranging from 0.9 μM to 9.9 mM containing 0.1 M KCl, 0.5 mM $\text{K}_3\text{Fe}(\text{CN})_6$ and 0.5 mM $\text{K}_4\text{Fe}(\text{CN})_6$ solution at scan rate 50 mV s^{-1} . (b) The relationship between logarithm of the concentration of NAM and the current response of $[\text{Fe}(\text{CN})_6]^{3-}/[\text{Fe}(\text{CN})_6]^{4-}$ on MIP-GCE

in the concentration range between $0.9 \times 10^{-6} \sim 9.9 \times 10^{-3}$ M (c) Binding isotherm of MIP electrode at different concentration of nicotinamide. Solid line-fitting curve for specific binding accompanied with non-specific adsorption.

Table 1. Comparison with other methods for the determination of NAM.

Moreover, in order to verify the performance and feasibility of the method, the MIP electrode was applied to the determination of NAM in a pharmaceutical product. A solution of a B-complex tablet, subsequently diluted to within range of the calibration plot was used. The samples were determined by a standard addition method. Differential pulse voltammograms were then recorded under the same conditions that were employed while recording differential pulse voltammograms for plotting calibration plot. The results showed that the recovery and relative standard deviations (RSD) (105.5% and 0.2, respectively) were acceptable and in good agreement with the manufacturer's stated contents of NAM, showing that the proposed method could be efficiently used for the analysis of NAM in pharmaceutical samples.

Selective recognition of the template molecule is an important parameter for a molecularly imprinted sensor.¹⁹ To examine the selectivity of the designed MIP electrode, some species having structures closely related to the imprinted molecules or substances that are present in biological/pharmaceutical products and may interfere with the determination of NAM through conventional methods, such as 4-amino-benzoic acid, Thiamine hydrochloride (Vitamin B₁), Riboflavin (Vitamin B₂), Pyridoxal (Vitamin B₆), Ascorbic acid (Vitamin C) were chosen as objective molecules to investigate the influence on the electrochemical responses of NAM in the molecularly imprinted electrochemical sensor. The change of current response of

$[\text{Fe}(\text{CN})_6]^{3-}/[\text{Fe}(\text{CN})_6]^{4-}$ on the MIP-GCE by DPV in a solution containing 25.0 μM NAM and various kinds of foreign compounds were detected using the MIP-GCE and the results are listed in Table 2. These results indicated that the imprinted OPPy-GC electrode showed higher recognition selectivity for NAM than for other compounds. This may be explained by the fact that the recognition sites formed in the imprinted PPy membranes had the capability to distinguish target molecules through their size, shape and functional group distribution.

The fabrication reproducibility of the imprinted OPPy-GC electrodes was estimated by determining the NAM level using three electrodes made independently under identical experimental conditions. The relative standard deviation (RSD) was 1.3% at NAM concentration of 45.0 μM . The repeatability of the sensor was investigated for 10.0 μM , as well. The calculated RSD was about 8% ($n = 5$).

Table 2. Effect of foreign substances on the detection of 25.0 μM NAM using the MIP-GCE.

4. CONCLUSION

We report a potential-gated electrochemical sensor using a molecularly imprinted polymer electrode for the determination of nicotinamide, which has improved qualities such as simple and low cost of preparation, a wide linear range, a low detection limit, high selectivity and stable modification of the electrode. NAM-imprinted overoxidised polypyrrole thin films were prepared by electropolymerisation of pyrrole in the presence of NAM as template on glassy carbon electrodes in aqueous solution. Preparation conditions affecting the MIP-GCE were optimised. The electrochemistry of a ferro/ferricyanide probe was used to monitor both template

removal and subsequent analyte binding. The prepared sensor exhibited a fast rebinding capacity and a good selective recognition of the template. Therefore, the application of imprinted PPy membranes as recognition elements, combined with electrochemical detection, shows promise for the detection of NAM in a complex matrix without separation.

Acknowledgments

The authors wish to acknowledge the Swedish Research Council (VR-2011-6058357) and Ferdowsi University of Mashhad, Iran for generous financial support to carry out this research.

Notes and references

Electronic Supplementary Information (ESI) available: [details of any supplementary information available should be included here]. See DOI: 10.1039/b000000x/

1. O. Parlak, A. P. F. Turner, A. Tiwari, *Advanced Materials*, 2014, **26**, 482-486.
2. a) A. Tiwari, H. Kobayashi, (Eds.), *Responsive Materials and Methods*; Wiley-Scrivener, USA, 2013; b) A. Tiwari, M. M. Demir (Eds.), *Advanced Sensor and Detection Materials*; Wiley-Scrivener, USA, 2014.
3. I. Y. Galaev, B. Mattiasson, *Trends Biotechnol.*, 1999, **17**, 335-340.
4. B. Jeong, A. Gutowska, *Trends Biotechnol.*, 2002, **20**, 305-311.
5. N. Karimian, M. H. Arbab Zavar, M. Chamsaz, A. P. F. Turner, A. Tiwari, *Electrochem. Commun.*, 2013, **36**, 92-95.
6. A. J. Hodgson, K. Gilmore, C. Small, G. C. Wallace, I. L. Mackenzie, T. Aoki, N. Ogata, *Supramolecular Science*, 1994, **1**, 77-83.

7. D. D. Ateh, H. A. Navsaria, P. Vadgama, *J. R. Soc. Interface*, 2006, **3**, 741-752.
8. J. Wang, M. Musameh, *Anal. Chim. Acta*, 2005, **539**, 209-213.
9. S. P. Özkorucuklu, Y. Şahin, G. Alsancak, *Sensors*, 2008, **8**, 8463-8478.
10. X. Kan, T. Liu, H. Zhou, C. Li, B. Fang, *Microchim. Acta*, 2010, **171**, 423-429.
11. A. Tiwari, S. R. Deshpandea, H. Kobayashi, A. P. F. Turner, *Biosens. Bioelectron.*, 2012, **35**, 224-229.
12. A. Tiwari, M. Ramalingam, H. Kobayashi, A. P. F. Turner, (Eds.), *Biomedical Materials and Diagnostic Devices*; Wiley-Scrivener, USA, 2012.
13. N. Karimian, M. Vagin, M. H. Arbab Zavar, M. Chamsaz, A. P. F. Turner, A. Tiwari, *Biosens. Bioelectron.*, 2013, **50**, 492-498.
14. A. Yarman, A. P. F. Turner, F. Scheller, In *Nanosensors for chemical and biological applications*; Honeychurch K. C., Ed.; Woodhead, 2014; pp 125-149.
15. K. Maiese, Z. Z. Chong, J. Hou, Y. C. Shang, *Molecules*, 2009, **14**, 3446-3485.
16. R. M. Kotkar, A. K. Srivastava, *J. Incl. Phenom. Macrocycl. Chem.*, 2008, **60**, 271-279.
17. R. D. Sole, M. R. Lazzoi, G. Vasapollo, *Drug Delivery*, 2010, **17**, 130-137.
18. S. Berchmans, R. Vijayavalli, *Bull. Electrochem.*, 1996, **12**, 411-414.
19. A. Ramanavicius, A. Ramanaviciene, A. Malinauskas, *Electrochim. Acta*, 2006, **51**, 6025-6037.
20. H. Ge, G. Qi, E. T. Kang, K.G. Neoh, *Polymer*, 1994, **35**, 504-508.
21. N. Karimian, A. P. F. Turner, A. Tiwari, *Biosens. Bioelectron.*, 2014, **59**, 160-165.
22. H. Munstedt, *Polymer*, 1986, **27**, 899-904.
23. A. Nezhadali, L. Mehri, R. Shadmehri, *Sens. Actuators B*, 2012, **171**, 1125-1131.

24. X. Kan, Z. Xing, A. Zhu, Z. Zhao, G. Xu, C. Li, H. Zhou, *Sens. Actuators B*, 2012, **168**, 395-401.
25. B. L. Li, J. H. Luo, H. Q. Luo, N. B. Li, *Sens. Actuators B*, 2013, **186**, 96-102.
26. C. Xie, S. Gao, Q. Guo, K. Xu, *Microchim. Acta*, 2010, **169**, 145-152.
27. A. I. Krasnova, M. P. Aguilar-Caballos, A. Gómez-Hens, *Anal. Chim. Acta*, 2001, **441**, 249-256.
28. A. Rafiq Khan, K. Mohammad Khan, S. Perveen, N. Butt, *J. Pharm. Biomed. Anal.*, 2002, **29**, 723-727.
29. R. D. Sole, A. Scardino, M. R. Lazzoi, G. Vasapollo, *J. Appl. Polym. Sci.*, 2011, **120**, 1634-1641.
30. I. Muszalska, K. Kiaszewicz, D. Kson, A. Sobczak, *J. Anal. Chem.*, 2013, **68**, 1007-1013.

Figure Captions

Scheme 1. Schematic representation of smart MIP surface via potentially tuned formation of the recognition site around template, NAM and specific NAM binding sites on the electrode.

Figure 1. Preparation of smart MIP electrode via electropolymerisation of pyrrole and template removal; (a) cyclic voltammogram for pyrrole electropolymerisation at a glassy carbon electrode (Py: 50.0 mM, NAM: 7.0 mM, sodium perchlorate: 100.0 mM in aqueous solution, number of cycles = 16, potential range -0.2 to +1.7 V and scan rate 100 mV s⁻¹). Inset: cyclic voltammograms recorded with bare GC electrode (black solid line, -I-) and MIP-modified (red dashed line, -II-) and NIP-modified (blue pointed line, -III-) electrodes in 0.5 mM K₃Fe(CN)₆, 0.5 mM K₄Fe(CN)₆, 0.1 M KCl; and (b) differential pulse voltammograms obtained with MIP (red solid line, -I-) and NIP-modified (blue dashed line, -II-) electrodes after template removing (cf., conditions are the same as inset of Fig. 1a). SEM images of c) MIP with insets of high resolution and d) NIP electrodes.

Figure 2. Optimization of factors affecting the performance of the smart MIP electrode; (a) effect of the pyrrole concentration on δi_p at the NAM/MIP-GCE; (b) effect of the cycles on δi_p at the NAM/MIP-GCE; (c) effect of the nicotinamide concentration on δi_p at the NAM/MIP-GCE; in the solutions containing 0.5 mM K₃Fe(CN)₆, 0.5 mM K₄Fe(CN)₆, 0.1 M KCl in the presence of 15.0 μ M nicotinamide after 10 min incubation time. (d) effect of the time of rebinding on δi_p at the NAM/MIP-GCE and NIP-GCE (cf., conditions are the same as Fig. 2 (a-c) just after different incubation times).

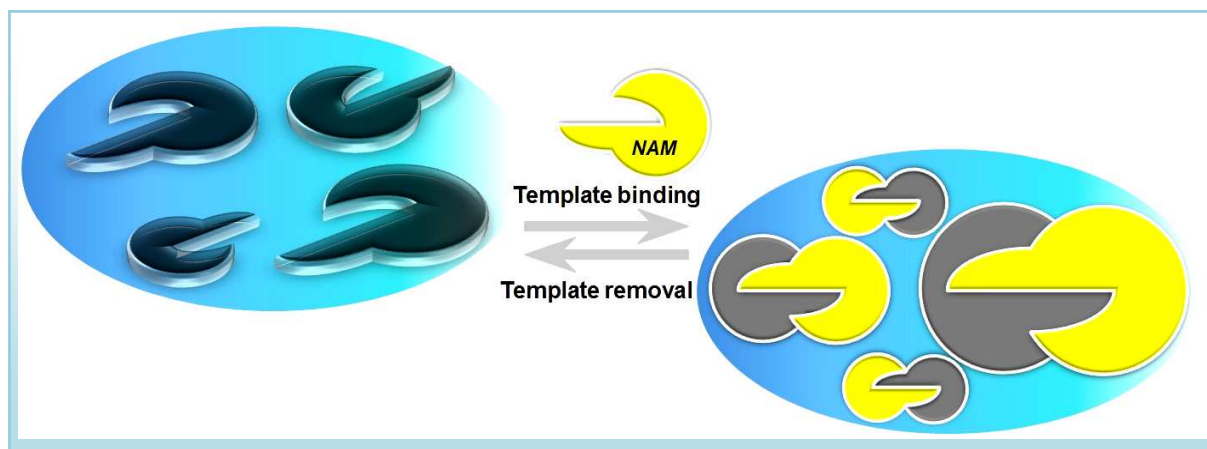
Figure 3. NAM binding with modified electrode. (a) Differential pulse voltammograms of MIP-modified electrode after 10 min of incubation in different NAM concentrations ranging from 0.9 μ M to 9.9 mM containing 0.1 M KCl, 0.5 mM $\text{K}_3\text{Fe}(\text{CN})_6$ and 0.5 mM $\text{K}_4\text{Fe}(\text{CN})_6$ solution at scan rate 50 mV/s. (b) The relationship between logarithm of the concentration of NAM and the current response of $[\text{Fe}(\text{CN})_6]^{3-}/[\text{Fe}(\text{CN})_6]^{4-}$ on MIP-GCE in the concentration range between $0.9 \times 10^{-6} \sim 9.9 \times 10^{-3}$ M (c) Binding isotherm of MIP electrode at different concentration of nicotinamide. Solid line-fitting curve for specific binding accompanied with non-specific adsorption.

Table 1. Comparison with other methods for the determination of NAM.

Method	Calibration range (M)	Detection limit (M)	References
Luminescence	0.8×10^{-6} - 162.0×10^{-6}	2.4×10^{-7}	[²⁷]
High Performance Liquid Chromatography (HPLC)	0.9×10^{-4} - 278.0×10^{-6}	16.4×10^{-6}	[²⁸]
Modified carbon paste electrode	0.8×10^{-6} - 4.1×10^{-3}	2.4×10^{-7}	[¹⁶]
MIP-Solid Phase Extraction (MIP-SPE)	41.0×10^{-6} - 4.0×10^{-3}	1.4×10^{-7}	[²⁹]
Differential spectrophotometry	9.8×10^{-6} - 499.5×10^{-6}	3.3×10^{-7}	[³⁰]
Electrochemical smart MIP sensor	0.9×10^{-6} - 9.9×10^{-3}	1.7×10^{-7}	Present work

Table 2. Effect of foreign substances on the detection of 25.0 μM NAM using the MIP-GCE.

Foreign substance	Concentration (μM)	Change in current response (%)
Ascorbic acid (Vitamin C)	25.0	+2.0
Riboflavin (Vitamin B ₂)	25.0	+6.4
Pyridoxal (Vitamin B ₆)	25.0	-5.2
Thiamine hydrochloride (Vitamin B ₁)	125.0	-2.9
4-Aminobenzoic acid	250.0	+6.8



Scheme 1.

N. Karimian et al.

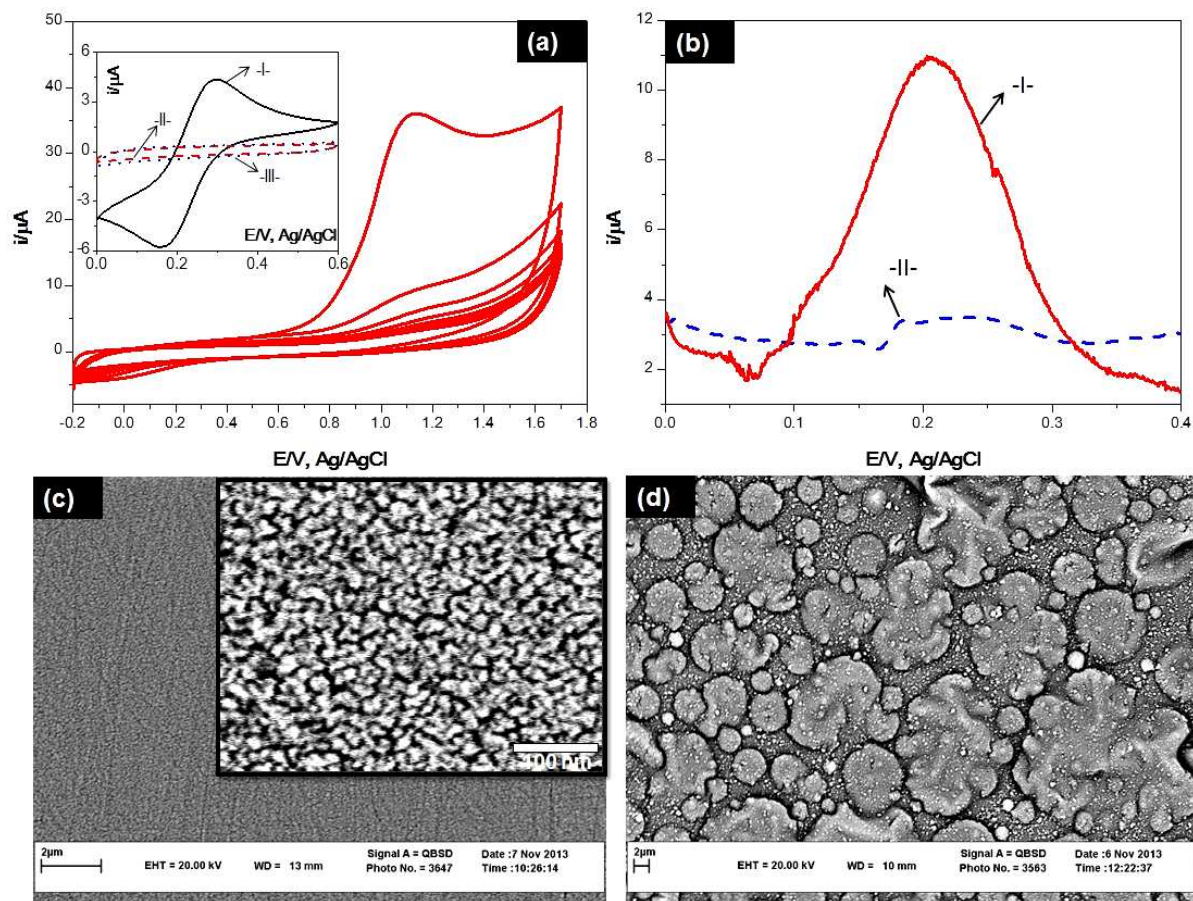
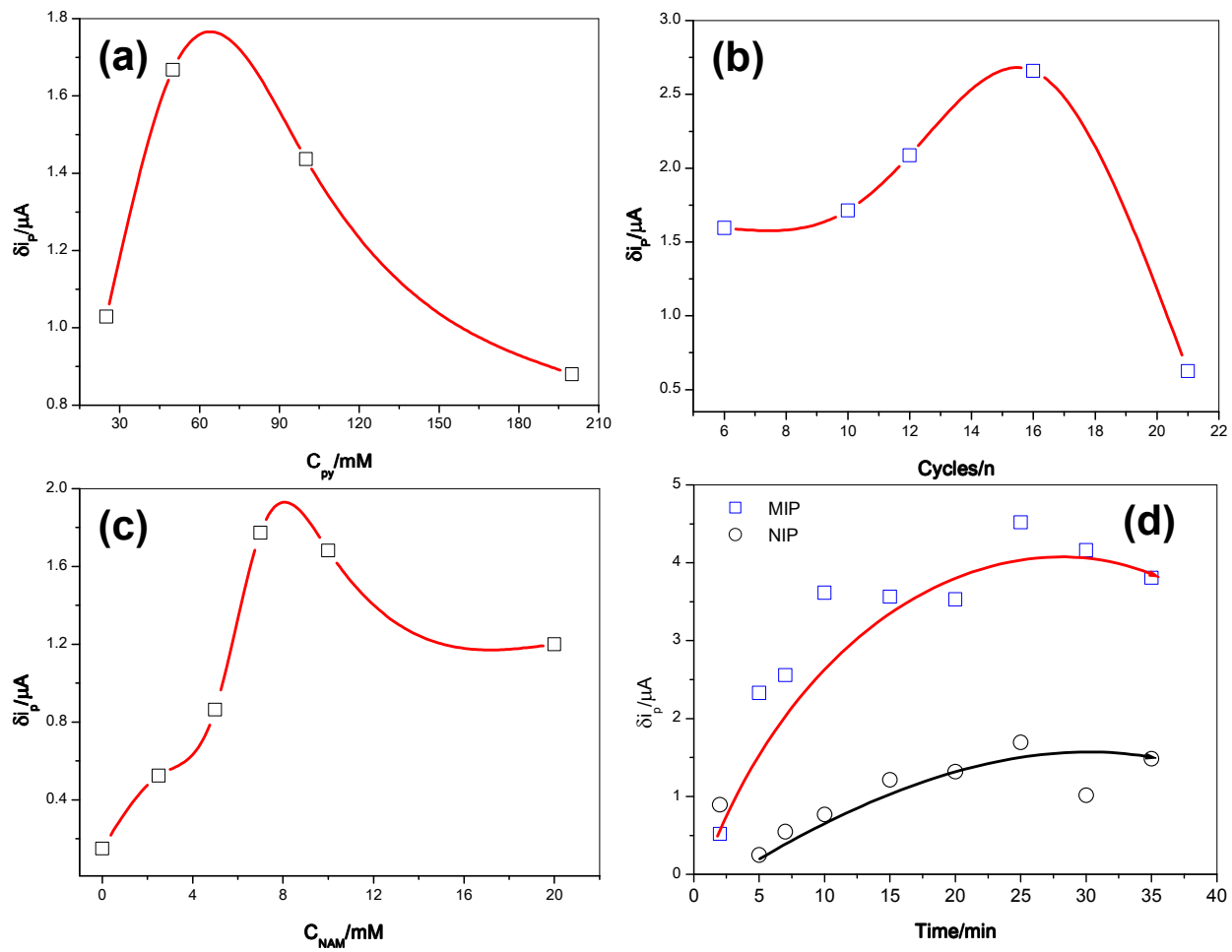


Figure 1.

N. Karimian et al.

**Figure 2.**

N. Karimian et al.

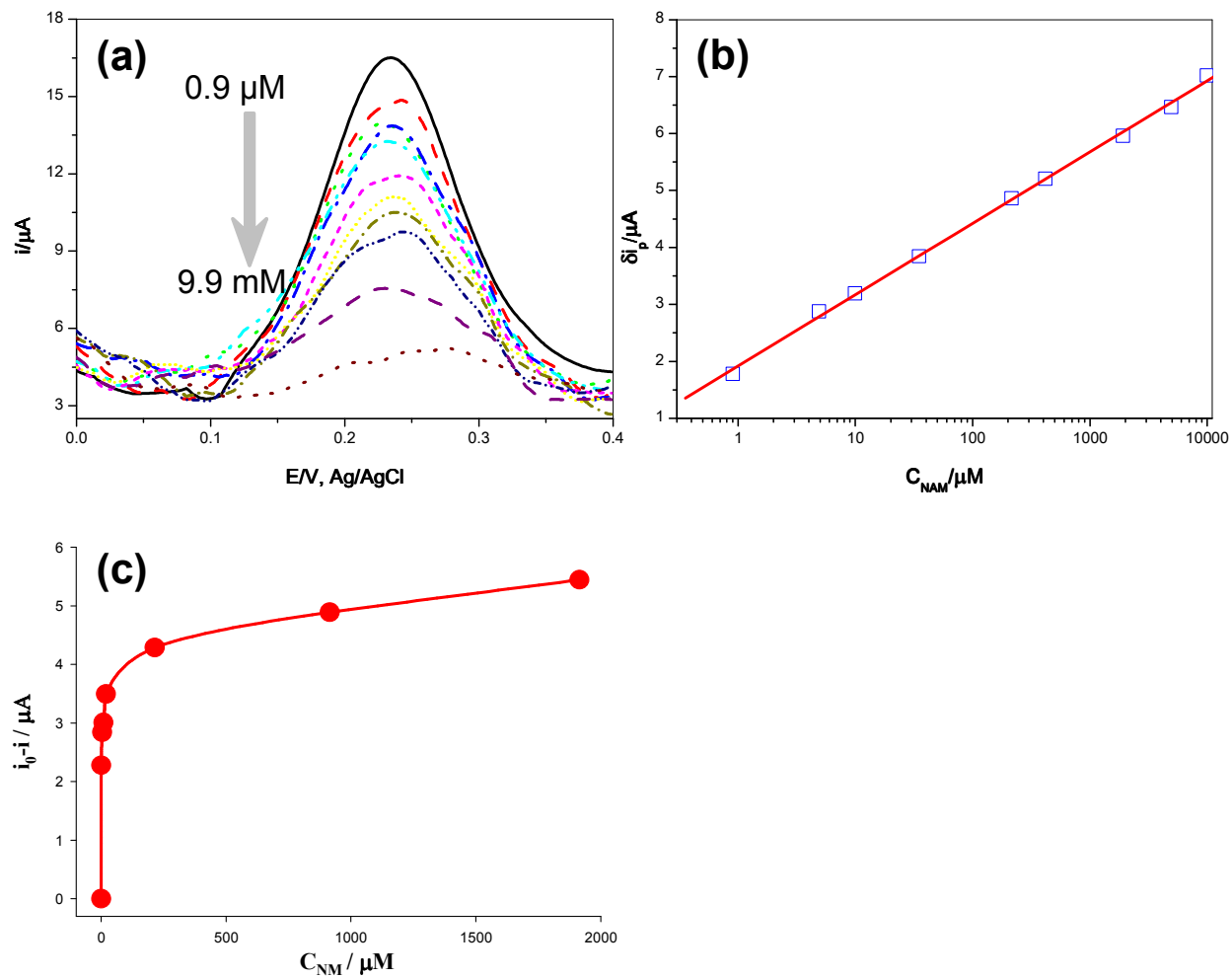


Figure 3.

N. Karimian et al.